9682 *Biochemistry* **2010,** *49,* 9682–9684
DOI: 10.1021/bi101507j

BIOCHEMISTRY
including biophysical chemistry & molecular biology
Rapid Report

Light-Induced Alteration of Low-Temperature Interprotein Electron Transfer between Photosystem I and Flavodoxin†

Lisa M. Utschig,* David M. Tiede, and Oleg G. Poluektov

Chemical Sciences and Engineering Division, Argonne National Laboratory, Argonne, Illinois 60439, United States

Received September 16, 2010; Revised Manuscript Received October 15, 2010

ABSTRACT: Electron paramagnetic resonance (EPR) was used to study light-induced electron transfer in Photosystem I−flavodoxin complexes. Deuteration of flavodoxin enables the signals of the reduced flavin acceptor and oxidized primary donor, P_{700}^{+}, to be well-resolved at X- and D-band EPR. In dark-adapted samples, photoinitiated interprotein electron transfer does not occur at 5 K. However, for samples prepared in dim light, significant interprotein electron transfer occurs at 5 K and a concomitant loss of the spin-correlated radical pair $P^{+}A_{1A}^{-}$ signal is observed. These results indicate a light-induced reorientation of flavodoxin in the PSI docking site that allows a high quantum yield efficiency for the interprotein electron transfer reaction.

Interprotein electron transfer reactions are involved in a variety of physiologically important processes. In photosynthesis, interprotein electron transfer reactions between mobile charge carrier proteins and integral membrane photosynthetic reaction center proteins (RCs) are essential for utilizing the photon energy, efficiently captured as a stabilized charge separation across the RC, to drive a series of cellular reactions, including $NADP^{+}$ reduction for carbon fixation (*1*). New experimental approaches for examining fundamentals of RC−charge carrier protein interactions can help discern factors involved in these dynamic protein−protein electron transfer events. Herein, we examine electron transfer between the Photosystem I reaction center protein (PSI) and its acceptor protein, flavodoxin.

PSI catalyzes light-driven electron transfer across the thylakoid membrane from plastocyanin located in the lumen to ferredoxin in the stroma (*2*). Flavodoxin replaces ferredoxin as an electron acceptor under iron deficiency in most cyanobacteria and some algae and is capable of substituting for ferredoxin in several ferredoxin-driven redox reactions, including reduction of ferredoxin-$NADP^{+}$ reductase (FNR) (*3*). Flavodoxin contains one flavin mononucleotide (FMN) cofactor and is capable of performing two successive single-electron transfer reactions, with the FMN group shuttling between the oxidized, protonated semiquinone, and fully reduced quinol redox states.

The photoreduction kinetics of ferredoxin and flavodoxin by PSI have been studied with optical spectroscopy (*1*, *4*). In addition, chemically cross-linked PSI−ferredoxin and PSI−flavodoxin complexes have been examined (*5*, *6*), and low-resolution crystal data have been obtained for a cocrystal of the PSI−ferredoxin complex (*7*). However, no detailed EPR spectroscopic studies of the light-induced electron transfer from PSI to its acceptor proteins in solution have been reported. In this paper, we demonstrate that EPR signals can be used to directly monitor the coupled interprotein electron transfer reaction that follows charge separation in the RC and report the observation of light-induced changes that alter electron transfer.

Following photoexcitation, a cascade of electron transfer events occurs between redox cofactors embedded within PSI (Figure 1A) (*2*). The primary electron donor of PSI, P_{700} (a dimer of chlorophyll molecules), becomes oxidized, with concurrent rapid, sequential electron transfer to two spectroscopically identified electron acceptors, A_0, a chlorophyll molecule, and A_1, a phylloquinone. From A_1^{-}, the electron is transferred to the [4Fe-4S] cluster F_X, and further to F_A and F_B, two [4Fe-4S] clusters held within the PsaC subunit. The electron is then transferred to either the [2Fe-2S] cluster of ferredoxin or the FMN cofactor of flavodoxin (*4*). EPR detection of ferredoxin photoreduction by PSI is complicated because the EPR signals of the reduced [2Fe-2S] cluster of ferredoxin and reduced [4Fe-4S] clusters of PSI are similar (*7*, *8*). Likewise, the *g* factors for oxidized P_{700}^{+} and the semiquinone radical of reduced protonated flavodoxin are similar and their EPR spectra strongly overlap when recorded via conventional X-band (9.5 GHz) EPR. However, deuteration of flavodoxin effectively narrows the inhomogeneous line width of the EPR signal that is due to unresolved hyperfine interactions (*9*, *10*). Figure 1B shows the D-band (134 GHz) high-field (HF) EPR spectrum of the semiquinone FMN radical for deuterated flavodoxin isolated from *Synechococcus lividus* grown in deuterated medium and purified with protonated buffers (*9*). The semiquinone state was generated by UV illumination of isolated flavodoxin in the presence of EDTA under anaerobic conditions. The substitution of ^{2}H at all nonexchangeable proton positions results in a decrease in the hydrogen hyperfine coupling constants so that the large coupling constants to nitrogens and exchangeable hydrogen are observed (*10*) and the flavodoxin semiquinone (Fld^{-}) signal can be easily distinguished from that of the oxidized protonated P_{700}^{+} via X-band EPR. The resolution of these signals is even better in D-band EPR spectra because of the high spectral resolution of HF EPR and small differences in the **g** tensors of Fld^{-} ($g_{xx} = 2.00436$; $g_{yy} = 2.00361$; $g_{zz} = 2.00221$) and P_{700}^{+} ($g_{xx} = 2.00329$; $g_{yy} = 2.00282$; $g_{zz} = 2.00246$).

We have used EPR spectroscopy to directly examine the photoinitiated interprotein electron transfer reaction between PSI and flavodoxin. A remarkable light dependence on the photoreduction of oxidized flavodoxin by PSI at cryogenic temperatures was observed. For these experiments, PSI isolated from cyanobacterial membranes of protonated *S. lividus* or *Synechococcus leopoliensis* (*11*) was incubated with deuterated *S. lividus* flavodoxin (*9*) in the presence of dichloro(phenol)indophenol (DCPIP) and

†This work is supported by the Division of Chemical Sciences, Geosciences, and Biosciences, Office of Basic Energy Sciences of the U.S. Department of Energy, under Contract DE-AC02-06CH11357.

*To whom correspondence should be addressed. E-mail: utschig@anl.gov. Phone: (630) 252-3544. Fax: (630) 252-9289.

 Published on Web 10/20/2010

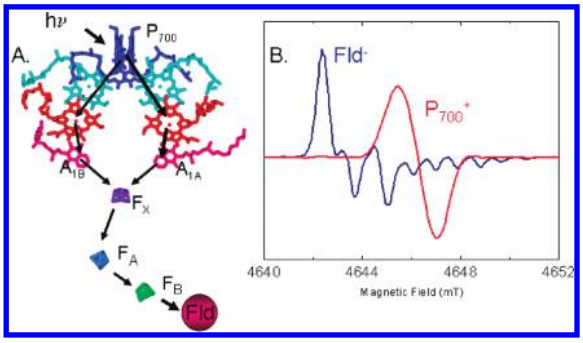

FIGURE 1: (A) Donor and acceptor cofactors and light-induced sequential electron transfer pathways of PSI. Following electron transfer through the terminal [4Fe-4S] clusters of PSI, interprotein electron transfer to either ferredoxin or flavodoxin (Fld) occurs. (B) D-Band (130 GHz) two-pulse, echo-induced field swept (ESE) EPR spectrum of deuterated flavodoxin recorded at 40 K (blue). The semiquinone state of isolated flavodoxin was generated by UV illumination in the presence of EDTA. This signal is distinct from that of the primary donor P_{700}^+ (red).

sodium ascorbate as donors to P_{700}^+. Figure 2A shows X-band EPR spectra for a sample prepared anaerobically in the dark prior to being frozen in liquid nitrogen. No EPR signal is observed in the initial dark spectrum. Following continuous illumination at 5 K, a signal due to P_{700}^+ is observed in the $g = 2.0$ region of the EPR spectrum. Signals of F_A^- and F_B^- are observed in a broader spectral window (data not shown). A Fld^- signal is not observed, indicating that no low-temperature interprotein electron transfer occurred in the strictly dark-adapted sample. Figure 2B shows EPR spectra for a sample that was exposed to dim room light (~4 μE m^{-2} s^{-1}) for 30 min at room temperature prior to being frozen in liquid nitrogen. For this light-exposed sample, a small Fld^- signal is observed in the initial dark spectrum. The intensity of this signal depends on the amount of light exposure prior to freezing. Following continuous illumination at 5 K, large overlapping signals of P_{700}^+ and Fld^- appear. Corresponding light-minus-dark EPR spectra obtained at the D-band for dark-adapted and light-exposed samples are shown in Figure 2C. As with the X-band spectra, only a P_{700}^+ signal is observed for the dark-adapted sample whereas signals from both P_{700}^+ and Fld^- are observed for the light-exposed sample.

X- and D-band EPR experiments provide definitive evidence that at room temperature a light-induced alteration that allows photoinitiated low-temperature interprotein electron transfer between PSI and flavodoxin occurs. What is the nature of the light-induced change? In general, electron transfer between proteins is facilitated by formation of a complex of two proteins, a dynamic process involving creation of an initial collision complex followed by additional rearrangement of the proteins into optimized conformations for electron transfer (*12*). Electrostatic alignment is a major determinant involved in orienting flavodoxin on PSI, with flavin atoms contributing (*3*, *13*−*15*). Our EPR results suggest an intriguing scenario in which, after the initial formation of a complex, the redox state of FMN directs the reorientation of flavodoxin within the PSI docking site. Under strict dark conditions, oxidized flavodoxin tests different docking positions on PSI. These PSI−Fld_{ox} conformations trapped by freezing are inactive with respect to low-temperature electron transfer. However, when in these PSI−Fld_{ox} conformations, flavodoxin can accept electrons via PSI light-induced room-temperature electron transfer under low-light conditions, and a pool of flavodoxin in the semiquinone state forms (Fld_{sq}). This Fld_{sq} reorients on the PSI surface to form a

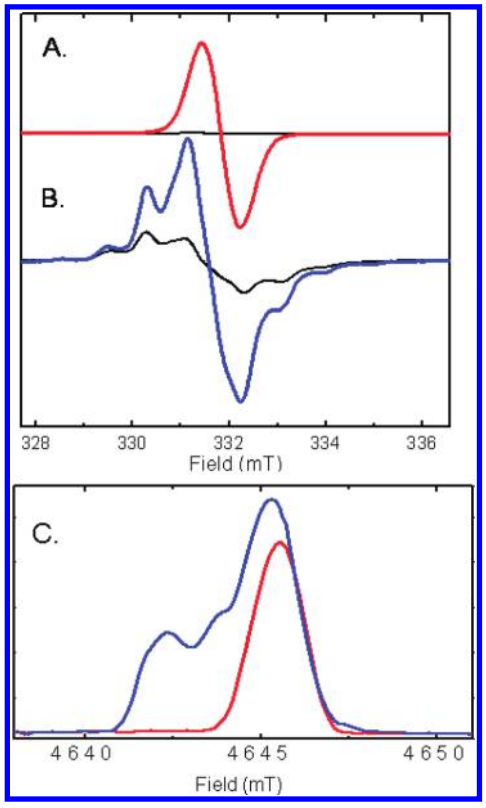

FIGURE 2: X-Band (9.5 GHz) continuous wave EPR spectra recorded at 5 K for PSI−flavodoxin samples that were either (A) strictly dark-adapted or (B) exposed to dim light at room temperature for 30 min prior to being frozen in liquid N_2. The sample contained 120 μM *S. leopoliensis* PSI, 840 μM *S. lividus* [^{2}H]flavodoxin, 10 mM ascorbate, 0.3 mM DCPIP, 20 mM Hepes (pH 7.8), 10 mM NaCl, 30 mM $MgSO_4$, 10 mM KCl, and 0.3% *n*-dodecyl β-D-maltopyranoside. Initial dark signals (black) and light-induced signals obtained by in-cavity illumination with a 200 W xenon lamp at 5 K are shown (red in panel A and blue in panel B). (C) D-Band (130 GHz) pulsed ESE EPR spectra recorded at 20 K for a PSI−flavodoxin sample (169 μM *S. lividus* PSI and 1.19 mM [^{2}H]flavodoxin) either strictly dark-adapted (red) or exposed to dim light (blue) prior to being frozen. Light-minus-dark spectra are shown. Note that EPR spectra recorded in the pulse mode (C) are shown as the absorption lines.

low-energy optimized PSI−Fld_{sq} complex. The Fld_{sq} within the complex becomes oxidized prior to being frozen in our experiment but remains locked in the optimized PSI−Fld_{sq} conformation. When frozen, the optimized PSI−Fld_{sq} conformation is observed as active with respect to low-temperature interprotein electron transfer. In vivo, such "redox reorientation" may be important so that Fld_{sq} is in the optimal position to accept a second electron to form hydroquinone (Fld_{hq}), as the Fld_{sq}/Fld_{hq} pair ($E_{sq/hq} \sim -400$ mV) is believed to shuttle electrons between PSI and FNR (*3*). This scenario is distinct from the light-induced alteration of reaction kinetics in bacterial RCs, the so-called "Kleinfeld effect" (*16*).

Importantly, data analysis of the EPR spectrum for the light-exposed sample shows remarkably efficient low-temperature photoreduction of flavodoxin by PSI. The efficiency can be estimated from fitting of the HF pulsed EPR data (Figure 2C). Spectral analysis shows a nearly 1:1 formation of oxidized donor P_{700}^+ and reduced flavodoxin acceptor Fld^- (see the Supporting Information). The high efficiency of PSI electron transfer to a bound acceptor protein is surprising. In the absence of flavodoxin, PSI has complicated low-temperature electron transfer kinetics, with low yields of electron transfer to the F_A and F_B electron acceptors (*17*, *18*).

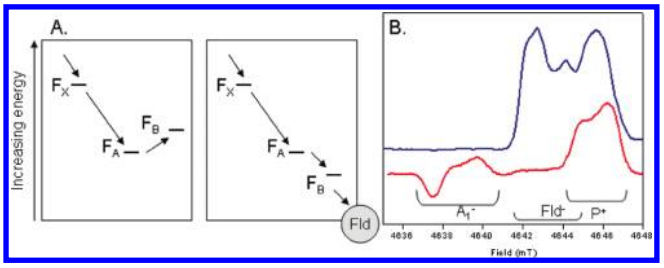

FIGURE 3: (A) Proposed change in redox potentials of the terminal [Fe-S] clusters of PSI after flavodoxin (Fld) binding. (B) D-Band time-resolved EPR spectra of PSI with (blue) or without (red) flavodoxin at 77 K. The initial dark signals (see the Supporting Information) were not subtracted from these spectra. The $P^+A_{1A}^-$ spin-correlated radical pair is observed for PSI but is absent in the presence of flavodoxin.

Our EPR results illustrate that, at low temperatures, PSI functions best when in a complex with its reaction partner. One idea is that flavodoxin binding alters the energetics of the terminal [Fe-S] clusters. In PSI, F_A has a more positive redox potential than F_B and electron transfer from F_A to F_B is uphill in terms of energy (*1*). This has been proposed to be a protective mechanism such that electron transfer from solvent-exposed F_B is not wasted by going to other molecules or detrimental oxygen (*19*). The observed 5 K interprotein electron transfer (Figure 2) provides evidence for a F_A to F_B downhill electron transfer step. Thus, our EPR results are consistent with the idea that, when flavodoxin is docked in the light-optimized complex on PSI, F_B is no longer exposed to solvent and F_B's redox potential changes to become more positive than that of F_A. With electron transfer from F_A to F_B being downhill in terms of energy, electron transfer to flavodoxin is facilitated (Figure 3A).

It is also possible that flavodoxin binding influences other electron transfer events within PSI. To investigate this, we examined time-resolved (TR) HF EPR spectra of PSI with and without flavodoxin bound. Electron transfer in PSI is bidirectional (for a review, see ref *20*), proceeding through two symmetric branches of cofactors, the A branch and the B branch (*21*). At low temperatures, a $P^+A_{1A}^-$ spin-correlated radical pair (SCRP) is routinely observed for PSI (*20*), as a fraction of electron transfer through the A branch of cofactors cannot proceed to F_X. A typical SCRP EPR signal of PSI (no flavodoxin) is shown in Figure 3B, with the P^+ and A_{1A}^- portions of the spectra clearly resolved at D-band. The TR spectrum of a PSI−flavodoxin solution exposed to dim light at room temperature prior to being frozen is also shown (Figure 3B). In this case, no SCRP is observed, most evident by the lack of signal in the quinone region of the HF spectrum. This result confirms the high efficiency of electron transfer through PSI in the presence of flavodoxin and, furthermore, suggests that both cofactor branches are open to electron transfer at low temperatures for dim light-exposed PSI−flavodoxin complexes.

In summary, EPR studies suggest light-induced redox reorientation of flavodoxin within the PSI docking site as a factor that influences the interprotein electron transfer event. Furthermore, we provide evidence that flavodoxin binding to PSI, in essence, completes the circuit of PSI electron transfer chemistry such that high-quantum yield efficiency is achieved for the interprotein electron transfer reaction at low temperatures.

ACKNOWLEDGMENT

This paper is dedicated to the memory of Henry L. Crespi, a pioneer in the deuteration of biological materials.

SUPPORTING INFORMATION AVAILABLE

Experimental methods for sample preparation, EPR measurements, and HF EPR data. This material is available free of charge via the Internet at http://pubs.acs.org.

REFERENCES

1. Golbeck, J. H. (2006) Photosystem I: The Light-Driven Plastocyanin: Ferredoxin Oxidoreductase, Springer, Dordrecht, The Netherlands.
2. Jordan, P., Fromme, P., Witt, H. T., Klukas, O., Saenger, W., and Krauss, N. (2001) *Nature 411*, 909–917.
3. Medina, M. (2009) *FEBS J. 276*, 3942–3958.
4. Sétif, P. (2001) *Biochim. Biophys. Acta 1507*, 161–179.
5. Lelong, C., Boekema, E. J., Kruip, J., Bottin, H., Rögner, M., and Sétif, P. (1996) *EMBO J. 15*, 2160–2168.
6. Mühlenhoff, U., Kruip, J., Bryant, D. A., Rögner, M., Sétif, P., and Boekema, E. J. (1996) *EMBO J. 15*, 488–497.
7. Fromme, P., Bottin, H., Krauss, N., and Sétif, P. (2002) *Biophys. J. 83*, 1760–1773.
8. Lelong, C., Sétif, P., Lagoutte, B., and Bottin, H. (1994) *J. Biol. Chem. 269*, 10034–10039.
9. Crespi, H. L., Norris, J. R., Bays, J. P., and Katz, J. J. (1973) *Ann. N. Y. Acad. Sci.,* 800–815.
10. Crespi, H. L., Norris, J. R., and Katz, J. J. (1971) *Biochim. Biophys. Acta 253*, 509–513.
11. Utschig, L. M., Chen, L. X., and Poluektov, O. G. (2008) *Biochemistry 47*, 3671–3676.
12. McLendon, G., and Hake, R. (1992) *Chem. Rev. 92*, 481–490.
13. Frago, S., Lans, I., Navarro, J. A., Hervás, M., Edmondson, D. E., De la Rosa, M. A., Gómez-Moreno, C., Mayhew, S. G., and Medina, M. (2010) *Biochim. Biophys. Acta 1797*, 262–271.
14. Goñi, G., Herguedas, B., Hervás, M., Peregrina, J. R., De la Rosa, M. A., Gómez-Moreno, C., Navarro, J. A., Hermoso, J. A., Martínez-Júlvez, M., and Medina, M. (2009) *Biochim. Biophys. Acta 1787*, 144–154.
15. Goñi, G., Serrano, A., Frago, S., Hervás, M., Peregrina, J. R., De la Rosa, M. A., Gomez-Moreno, C., Navarro, J. A., and Medina, M. (2008) *Biochemistry 47*, 1207–1217.
16. Kleinfeld, D., Okamura, M. Y., and Feher, G. (1984) *Biochemistry 23*, 5780–5786.
17. Brettel, K. (1997) *Biochim. Biophys. Acta 1318*, 322–373.
18. Schlodder, E., Flalkenberg, K., Gergeleit, M., and Brettel, K. (1998) *Biochemistry 37*, 9466–9476.
19. Shinkarev, V. P., Vassiliev, I. R., and Golbeck, J. H. (2000) *Biophys. J. 78*, 363–372.
20. Srinivasan, N., and Golbeck, J. H. (2009) *Biochim. Biophys. Acta 1787*, 1057–1088.
21. Poluektov, O. G., Paschenko, S. V., Utschig, L. M., Lakshmi, K. V., and Thurnauer, M. C. (2005) *J. Am. Chem. Soc. 127*, 11910–11911.